2010 IEEE International Conference on Robotics and Automation
Anchorage Convention District
May 3-8, 2010, Anchorage, Alaska, USA

# Approximations to Continuous Curves of Active Cord Mechanism Made of Arc-shaped joints or Double Joints

Hiroya Yamada and Shigeo Hirose

*Abstract*— **In this paper, we discuss approximations to continuous curves of the Active Cord Mechanism (ACM) which is composed of arc-shaped joints or double joints. ACM is a machine which is made of a series of bending joints and forms a cord, and it has potential to work in challenging environment due to its large degree of freedom. In prior research most of ACM were composed of straight links and joints, and a lot of successful control methods for them have been proposed. However, the control of the ACM that is composed of arc-shaped joints or double joints has not been studied sufficiently so far. In this research we propose the method of approximations to continuous curves for such kind of ACM and use it for the control. The proposed idea is verified by numerical calculations and experiments by a robot.**

## I. INTRODUCTION

Active Cord Mechanism (ACM) is a machine inspired by a snake. It is defined as " a functional body which connects in a series joint units, and which forms a cord"[1]. ACM is a unique system because it has can have extremely large number of degree of freedom but it is easily realized by just connecting same bending joints in series. Thanks to this unique feature, ACM has been studied as one of hopeful kind of robots for tasks in challenging environments.

A typical ACM in prior research is composed of straight links connected by revolute joints, and its degree of freedom is the same with the number of the joints. This structure is simple and suitable for the design using rotary actuators, but it has following demerits: One is that the shape is not smooth when the joint angles are large. The other is that the range of motion is limited by collision between links, particularly in case of universal joints.

In addition to the above mechanism, a joint bending like an arc has been proposed[2][3] (we call it an arc-shaped joint in this paper). The example of an arc-shaped joint is shown in Fig. 1. It is made up of an elastic element, 2 disks and 3 cables, and the pulling force of cable bends the element like an arc. An arc-shaped joint is ideal for ACM because its shape is smooth if it bends with large angle. However, it is difficult to design a compact arc-shaped joint with rotary actuators, so the application for ACM is not many in prior research.

Recently we have focused on a double joint as another type of joint for ACM. In this paper we define a "double joint" as a joint which has 2 rotating axis for 1 DOF and its rotational angles around the 2 axes are the same. For example, a double joint which bend around pitch and yaw axis can be realized by 2 differential mechanisms connected by pulleys and cables as shown in Fig. 2[4]. A double joint has smooth bending shape like an arc-shaped joint, and it is feasible to design a compact joint using rotary actuators.

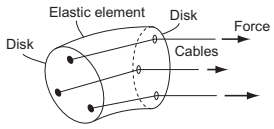


Fig. 1. Example of an arc-shaped joint

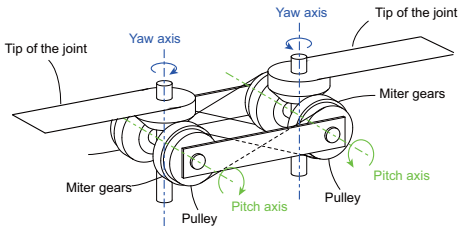


Fig. 2. Example of a double joint

However, the control of ACM which is composed of arc-shaped joints or double joints has not been studied enough. Thus we propose the control method based on approximation to a continuous curve, which have been used for previous robots composed of straight links[5]. In this control method, the motion is generated by continuous model, and at the same time the robot is controlled to approximate that motion as shown in Fig. 3. The merit of this method is that we can study the motion of ACM with a general ideal model and apply it to various mechanisms. In this paper we discuss the method of approximations to continuous curves of ACM composed of arc-shaped joints or double joints, which is the key of the proposed control method.

This paper is organized as follows: Section II describes the definition of continuous model of ACM and approximations by ACM composed of straight links. Section III and IV present the approximations by ACM composed of arc-shaped joints and double joints respectively. Section V presents the experiment of a robot composed of double joints, and Section VI gives the conclusion.

This work was not supported by any organization

H. Yamada is with Global Edge Institute, Tokyo Institute of Technology, 2-12-1 Ookayama, Meguro-ku, Tokyo, Japan yamada@robotics.mes.titech.ac.jp

S. Hirose is with Department of Mechanical and Aerospace Engineering, Tokyo Institute of Technology, 2-12-1 Ookayama, Meguro-ku, Tokyo, Japan Hirose@mes.titech.ac.jp

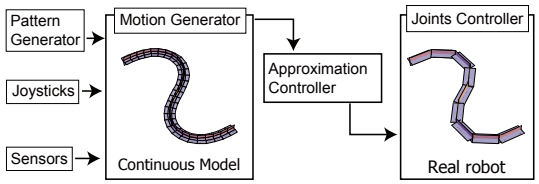


Fig. 3. The control based on the continuous model of ACM

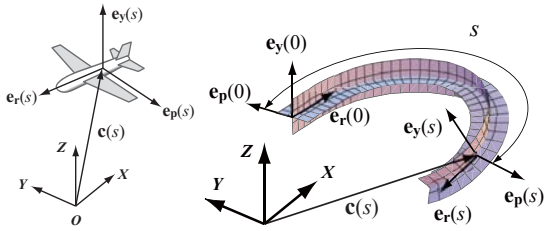


(a) Analogy with aircraft (b) A dorsal reference curve

Fig. 4. A dorsal reference curve

## II. PRIOR RESEARCH

### A. Dorsal reference curve

A continuous curve is not enough to represent the shape of continuous ACM, because ACM has the body which has the distinction of the belly and the back[6]. Thus we have introduced differential equations extended from Frenet-Serret equations of a spatial curve, and called the solution as "dorsal reference curve" and applied it to the study of ACM[7][8][9]. A dorsal reference curve is a natural representation of an elongate body, in fact the same idea was introduced for the study of elastica in the field of physics in 19th century[10].

A dorsal reference curve is explained by analogy of a track of an air plane (Fig. 4(a)). First we consider a vector $\mathbf{c} = (x(s), y(s), z(s))$ as the position of the plane. $s$ is a length of the track, and $s = 0$ means the starting point. An orthogonal frame $(\mathbf{e}_r(s), \mathbf{e}_p(s), \mathbf{e}_y(s))$ is considered as the posture of the plane, and $\mathbf{e}_r(s)$ (roll axis) is a unit vector facing the moving direction of the plane, $\mathbf{e}_p(s)$ (pitch axis) is a unit vector facing to the direction of the left wing, and $\mathbf{e}_y(s)$ (yaw axis) is a unit vector facing to the direction of the vertical tail.

The plane has an aileron, an elevator, and a rudder so we introduce 3 functions $\tau(s)$, $\kappa_p(s)$ and $\kappa_y(s)$ as the rotational velocity of rolling, pitching, and yawing motion respectively. We think these function means the difference of rotational angle [rad] when the plane travels for a unit length. Now the track of the plane is calculated by following equations[7][8].

$$\begin{cases} \dfrac{d\mathbf{c}(s)}{ds} &= \mathbf{e}_r(s) \\ \dfrac{d\mathbf{e}_r(s)}{ds} &= \kappa_y(s)\mathbf{e}_p(s) - \kappa_p(s)\mathbf{e}_y(s) \\ \dfrac{d\mathbf{e}_p(s)}{ds} &= -\kappa_y(s)\mathbf{e}_r(s) + \tau(s)\mathbf{e}_y(s) \\ \dfrac{d\mathbf{e}_y(s)}{ds} &= \kappa_p(s)\mathbf{e}_r(s) - \tau(s)\mathbf{e}_p(s) \end{cases} \tag{1}$$

If the position $(\mathbf{c}(0))$ and the posture $(\mathbf{e}_r(0), \mathbf{e}_p(0), \mathbf{e}_y(0))$ at the starting point $(s = 0)$ and $\tau(s), \kappa_p(s), \kappa_y(s)$ are given, the position $(\mathbf{c}(s))$ and the posture $(\mathbf{e}_r(s), \mathbf{e}_p(s), \mathbf{e}_y(s))$ on the track are obtained as the solution of (1). Fig. 4(b) shows a visualized image of a solution.

Now we consider the starting point of the track as the head (or tail) of an ACM, and consider $\mathbf{c}(s)$ as the position of the body, and consider $(\mathbf{e}_r(s), \mathbf{e}_p(s), \mathbf{e}_y(s))$ as the posture of the body. Thus we can translate the track to the shape of the ACM. We call the set of $\mathbf{c}(s)$ and $(\mathbf{e}_r(s), \mathbf{e}_p(s), \mathbf{e}_y(s))$ a "dorsal reference curve", because its shape (Fig. 4(b)) reminds us a slender fish that has a dorsal fin. In addition we call $\tau(s), \kappa_p(s), \kappa_y(s)$ shape functions.

### B. Approximation of a link model

We have proposed a method to approximate a dorsal reference curve by an ACM composed of straight links (here we call it straight link model), in which the joint angles of the straight link model are calculated by integrating the shape functions (see [5] for the detail). For example, we think a straight link model which is composed of links with the same length, and the links are alternatively connected by yawing joints and pitching joints (Fig. 5). This straight link model doesn't have rolling joint, so it can approximate only dorsal reference curves with $\tau(s) = 0$. In that method, the joint angles are calculated as following.

$$\theta_{p,i} = \int_{l\cdot(i-1)}^{l\cdot(i+1)} \kappa_p(l \cdot i)ds \tag{2}$$

$$\theta_{y,i} = \int_{l\cdot(i-1)}^{l\cdot(i+1)} \kappa_y(l \cdot i)ds \tag{3}$$

Here $\theta_{p,i}$, $\theta_{y,i}$ are a pitching angle and yawing angle of the $i$-th joint respectively, and $l$ is the length of a link. However, we consider $\theta_{y,i} = 0$ if the $i$-th joint is pitching joint, and vice versa. In addition we think that there is a virtual joint (0th joint) at the tip, and $\kappa_p(s) = \kappa_y(s) = 0$ at $s < 0$. Fig. 6 shows the approximation results of a serpenoid, which expresses the shape of serpentine movement of a snake, and spatial spiral. The shape functions of the serpenoid are given as follows:

$$\kappa_p(s) = 0, \quad \kappa_y(s) = \frac{2\pi\alpha}{L}\sin(\frac{2\pi}{L}s) \tag{4}$$

In this paper $\alpha = \pi/3$, and $L$ is the same with the total length of a model. The functions of a spiral are as follows[8]:

$$\begin{aligned} \kappa_p(s) &= -\kappa_c \sin(\tau_c s) \\ \kappa_y(s) &= \kappa_c \cos(\tau_c s) \end{aligned} \tag{5}$$

We set $\kappa_c = 12/L_t$, $\tau_c = 3.6/L_t$ in this paper, where $L_t$ is the total length of a model.

We use the following function to evaluate the error of approximations[5].

$$E_{nm} = \frac{\int_0^{L_t} \parallel \mathbf{c}(s) - \mathbf{c}_d(s) \parallel ds}{L_t^2} \tag{6}$$

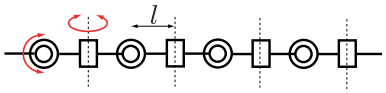


Fig. 5. A typical structure of a straight link model

$\mathbf{c}_d(s)$ is a vector of the position of a model to evaluate such as a straight link model or an arc-shaped joint model or a double joint model. $E_{nm}$ means a ratio of average distance between 2 models to $L_t$. Thus if we set the same starting position and posture for both model, the better the approximation becomes, the smaller $E_{nm}$ becomes.

The principle of this method is explained using an example of a planar curve (a curve with $\tau(s) = \kappa_p(s) = 0$) as follows: First, we define 2 functions as follows:

$$\phi_y(s) \equiv \int_0^s \kappa_y(s)ds \tag{7}$$

$$\phi_{ly}(s) \equiv \sum_{i=0}^{\mathrm{floor}(s/l)} \theta_{y,i} \tag{8}$$

$\mathrm{floor}(x)$ is floor function, that means the largest integer not greater than $x$. $\phi_y(s)$ means the angle between $\mathbf{e}_r(0)$ and the tangential vector of the curve at $s$, and $\phi_{ly}(s)$ means the angle between $\mathbf{e}_r(0)$ and the link of the straight link model at $s$. Therefore if $\phi_y(s)$ and $\phi_{ly}(s)$ become close, the shapes of both models become similar. When we use (3), $\phi_{ly}(s)$ becomes a function that approximate $\phi_y(s)$ by steps as shown in Fig. 6(c), so the straight link model approximates the curve. Even in case of 3D curve we can define the same kind of functions as (7) and (8) for each shape functions, and we obtained the fact that this approach is available even in the case of 3D curve through numerical simulation.

## III. APPROXIMATION OF AN ARC-SHAPED JOINT MODEL

### A. A planar model

First, we discuss the way to approximate a planar curve by an arc-shaped joint model. We introduce a function which means the sum of bending angles as follows:

$$\phi_{ay}(s) \equiv \sum_{i=0}^{m} \theta_{ay,i} + \frac{(s - l_a \cdot m)}{l_a}\theta_{ay,m+1} \tag{9}$$

$$where \quad m = \mathrm{floor}(s/l_a) \tag{10}$$

Here $\theta_{ay,i}$ is the bending angle of $i$-th arc-shaped joint, and $l_a$ is the length of a joint. We think there is a virtual arc-shaped joint with length 0 at $s = 0$, and its angle is $\theta_{ay,0}$. The graph of $\phi_{ay}(s)$ becomes a line graph, and the tangent of each line is $\theta_{ay,i}/l_a$. When we set the starting point of a planar curve and an arc-shaped joint model as the same, $\phi_{ay}(s)$ means the angle between $\mathbf{e}_r(0)$ and the tangential vector of the arc-shaped joint model at $s$.

We expect an arc-shaped joint model would approximate a planar curve when $\phi_{ay}(s)$ becomes close to $\phi_y(s)$ as the result of a straight link model. We investigated various

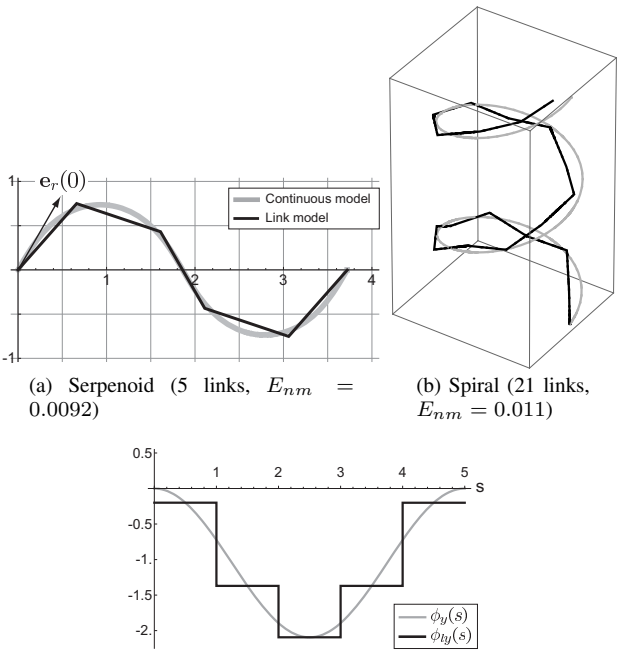


(a) Serpenoid (5 links, $E_{nm} = 0.0092$)

(b) Spiral (21 links, $E_{nm} = 0.011$)

(c) $\phi_y(s)$ and $\phi_{ly}(s)$ in case of the serpenoid

Fig. 6. Approximations by a straight link model

calculation rules by trial and error, and the following method was the best.

The process of this method is divided to 3 steps. At the first step, we calculate $\theta_{ay,i}$ that makes $\phi_{ay}(s)$ as the same with $\phi_y(s)$ at $s = l_c(1-p), l_cp, l_c(1+p), \cdots, l_c(n-1+p)$, and save it as $\theta^a_{ay,i}$. At the second step, we calculate $\theta_{ay,i}$ that makes $\phi_{ay}(s)$ as the same with $\phi_y(s)$ at $s = l_c(n-1+p), l_c(n-p), l_c(n-1-p), \cdots, l_c(1-p)$, and save it as $\theta^b_{ay,i}$. At the third step, we decide $\theta_{ay,i}$ as the average of $\theta^a_{ay,i}$ and $\theta^b_{ay,i}$. The actual calculation is as follows.

First step:

$$\theta^a_{ay,1} = \frac{1}{2p-1}\int_{(1-p)l_c}^{pl_c} \kappa(s)ds \tag{11}$$

$$\theta^a_{ay,i} = \frac{1}{p}\left\{\int_{(i-2+p)l_c}^{(i-1+p)l_c} \kappa(s)ds - \theta^a_{ay,i-1}(1-p)\right\} \cdots (i = 2, 3, \cdots, n) \tag{12}$$

$$\theta^a_{ay,0} = \int_0^{(1-p)l_c} \kappa(s)ds - (1-p)\theta^a_{ay,1} \tag{13}$$

Where $p$ is a parameter ($0.5 < p \leq 1$), and $n$ is the total number of arc-shaped joints.

Second step:

$$\theta^b_{ay,n} = \frac{1}{2p-1}\int_{(n-p)l_c}^{(n-1+p)l_c} \kappa(s)ds \tag{14}$$

$$\theta^b_{ay,i} = \frac{1}{p}\left\{\int_{(i-p)l_c}^{(i+1-p)l_c} \kappa(s)ds - \theta^b_{ay,i+1}(1-p)\right\} \cdots (i = n-1, n-2, \cdots, 1) \tag{15}$$

$$\theta^b_{ay,0} = \int_0^{(1-p)l_c} \kappa(s)ds - (1-p)\theta^b_{ay,1} \tag{16}$$

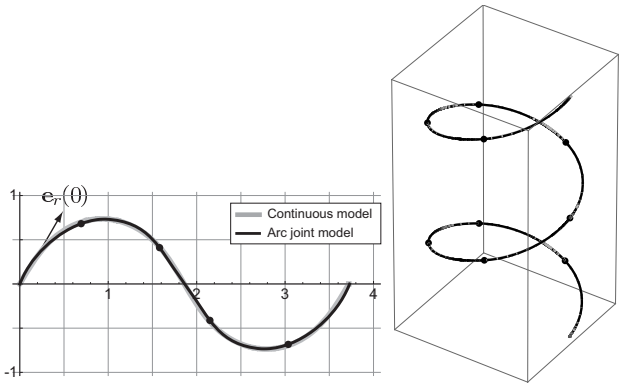


(a) Serpenoid (5 arcs, $E_{nm} = 0.0022$)



(b) Spiral (10 arcs, $E_{nm} = 0.00021$)

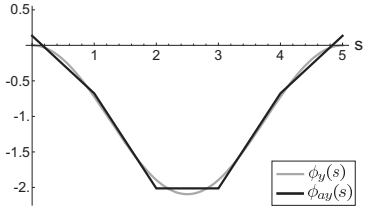


(c) $\phi_y(s)$ and $\phi_{ly}(s)$ in case of the serpenoid

Fig. 7. Approximations by an arc-shaped joint model

Third step:

$$\theta_{ay,i} = (\theta^a_{ay,i} + \theta^b_{ay,i})/2 \tag{17}$$

Parameter $p$ has a large influence on the approximation, and we conclude $p = 0.789$ is appropriate from numerical simulations. Fig. 7(a) shows the approximation of serpenoid of (4), and the error ($E_{nm}$) is only 1/4 of that of a straight link model in Fig. 6(a). In this case $\phi_{ay}(s)$ becomes successfully close to $\phi_y(s)$ as shown in Fig. 7(c).

### *B. 3D arc-shaped joint model*

We apply the method in former section to a 3D arc-shaped joint model, which is composed of arc-shaped joints bending to 2 directions at the same time as shown in Fig. 8. When we define $\theta_{a,i}$ as bending angle and $\psi_{a,i}$ as direction of bending, the difference of the frame is obtained as follows:

$$\begin{pmatrix} \mathbf{e}_{ar}(s_{i+1}) \\ \mathbf{e}_{ap}(s_{i+1}) \\ \mathbf{e}_{ay}(s_{i+1}) \end{pmatrix} = \mathbf{E}_r(-\psi_{a,i})\mathbf{E}_p(\theta_{a,i})\mathbf{E}_r(\psi_{a,i}) \begin{pmatrix} \mathbf{e}_{ar}(s_i) \\ \mathbf{e}_{ap}(s_i) \\ \mathbf{e}_{ay}(s_i) \end{pmatrix} \tag{18}$$

$\mathbf{E}_r(x)$ and $\mathbf{E}_p(x)$ are defined as follows:

$$\mathbf{E}_r(x) = \begin{pmatrix} 1 & 0 & 0 \\ 0 & \cos x & \sin x \\ 0 & -\sin x & \cos x \end{pmatrix} \tag{19}$$

$$\mathbf{E}_p(x) = \begin{pmatrix} \cos x & 0 & -\sin x \\ 0 & 1 & 0 \\ \sin x & 0 & \cos x \end{pmatrix} \tag{20}$$

Now we define the pitching angle and yawing angle of an arc-shaped joint in Fig. 8 as follows:

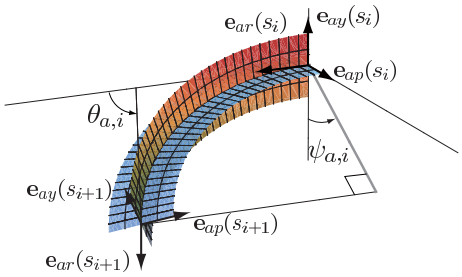


Fig. 8. The shape of a 3D arc-shaped joint

$$\theta_{ap,i} = \theta_{a,i}\cos\psi_{a,i} \tag{21}$$

$$\theta_{ay,i} = \theta_{a,i}\sin\psi_{a,i} \tag{22}$$

In approximation of a dorsal reference curve with $\tau(s) = 0$, we calculate $\theta_{ap,i}$ and $\theta_{ay,i}$ by (11) $\sim$ (17) ($\theta_{ap,i}$ is calculated by replacing the suffix "y" to "p"). Fig. 7(b) shows the approximation of spiral of (5) (The dorsal fin in Fig. 7(b) is omitted for the ease to see, but the dorsal fin of the arc-shaped joint model is also close to that of the dorsal reference curve). In addition we confirmed that this method is available for other curves .

## IV. APPROXMATION OF A DOUBLE JOINT MODEL

In the study of double joints for ACM, we have noticed an interesting similarity of double joints and arc-shaped joints. This similarity enables us to apply the approximation method described in Section III directly to a double joint model.

Now we consider a double joint on a plane as shown in Fig. 9(a). The total length of the joint is 1 and the length of links of both ends is $R_s$. When the bending angle of the joint is $\theta$, the position of the end of the joint is obtained as follows:

$$x_d(\theta) = (1-2R_s)\cos\frac{\theta}{2} + R_s(1+\cos\theta) \tag{23}$$

$$y_d(\theta) = (1-2R_s)\sin\frac{\theta}{2} + R_s\sin\theta \tag{24}$$

Then we consider an arc-shaped joint whose length is 1 and bending angle is $\theta$ as shown in Fig. 9(b). The position of its end is obtained as follows:

$$x_a(\theta) = \frac{\sin\theta}{\theta} \tag{25}$$

$$y_a(\theta) = \frac{1-\cos\theta}{\theta} \tag{26}$$

Fig. 10 shows the positions of the ends of both models in case of $R_s = 0.18$. It is interesting the distance between both ends is less than 1% of the total length when we set $R_s$ at $1.6 \sim 1.8$ and $-\pi/2 < \theta < \pi/2$. Thanks to this fact we can apply the approximation method of an arc-shaped joint model to a double joint model.

However, for a 3D model, the joint angle of a double joint should be calculated by inverse kinematics. Now we are going to replace an arc-shaped joint shown in Fig. 8

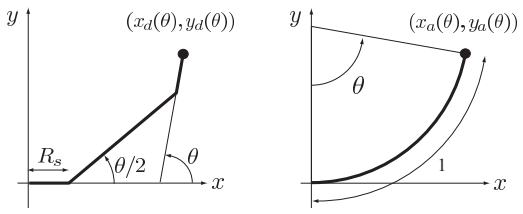


(a) A double joint (b) An arc-shaped joint

Fig. 9. The position of the tip of a joint

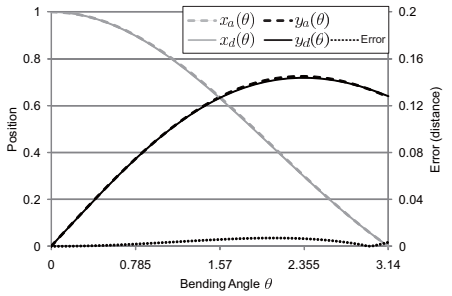


Fig. 10. Comparison of the tips of an arc-shaped joint and a double joint ($R_s = 0.18$)

by a double joint shown in Fig. 11. We consider a vector $\mathbf{u} = u_x\mathbf{e}_{ar}(s_i) + u_y\mathbf{e}_{ap}(s_i) + u_z\mathbf{e}_{ay}(s_i)$ as a direction vector of the central link of the double joint. When the order of rotating axes of the double joint is as the same with Fig. 2 (that is, yaw, pitch, pitch, yaw), $u$ is expressed as follows:

$$u_x = \cos(\theta_{dp,i}/2)\cos(\theta_{dy,i}/2) \quad (27)$$
$$u_y = \cos(\theta_{dp,i}/2)\sin(\theta_{dy,i}/2) \quad (28)$$
$$u_z = -\sin(\theta_{dp,i}/2) \quad (29)$$

Here $\theta_{dp,i}$, $\theta_{dy,i}$ are pitching and yawing angle of the $i$-th double joint respectively. On the other hand, $\mathbf{u}$ should be the tangential vector of the middle of arc-shaped joint, so the following equation should be true.

$$u_x = \cos(\theta_{a,i}/2) \quad (30)$$
$$u_y = \sin(\theta_{a,i}/2)\sin\psi_{a,i} \quad (31)$$
$$u_z = -\sin(\theta_{a,i}/2)\cos\psi_{a,i} \quad (32)$$

Then the following equation is derived from (29), (32), (21), (22).

$$\theta_{dp,i} = 2\sin^{-1}\{\sin(\theta_{a,i}/2)\cos\psi_{a,i}\} = 2\sin^{-1}\left\{\sin(\theta_{a,i}/2)\frac{\theta_{ap,i}}{\theta_{a,i}}\right\} \quad (33)$$

In addition the following equation is derived from (29), (32), (21), (22).

$$\theta_{dy,i} = 2\sin^{-1}\left\{\sin(\theta_{a,i}/2)\sin\psi_{a,i}\frac{1}{\cos(\theta_{dp,i}/2)}\right\} = 2\sin^{-1}\left\{\sin(\theta_{a,i}/2)\frac{\theta_{ay,i}}{\theta_{a,i}}\frac{1}{\cos(\theta_{dp,i}/2)}\right\} \quad (34)$$

The approximation by a double joint model is conducted by calculating the angles of an arc-shaped joint model with method in Section III and using (33), (34). Fig. 12 shows the approximation of serpenoid (4) and spiral (5). The error is larger than that of the arc-shaped joint model, but smaller than that of the straight link model.

## V. EXPERIMENT

### A. Structure of a robot "ACM-L2"

We verified the proposed method by experiments with a robot "ACM-L2"[4], which was composed of double joints. Table I shows the specification of ACM-L2. The length of each joint is 78 mm and the length of central link is 50mm, so $R_s$ in (23) is 0.18.

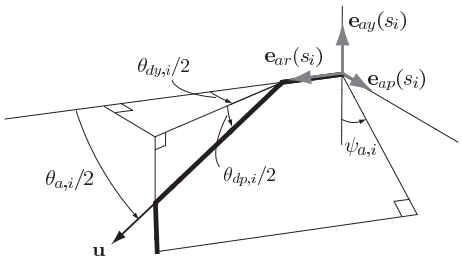


Fig. 11. Direction of the center link of a double joint

The control system is composed of a PC which generates the motion of the whole body, and microcomputers which control the angles of each joints. The PC program deals with the shape functions of a dorsal reference curve as arrays, and generates the motion of the curve. The shape of the dorsal reference curve is converted to joint angles by the proposed method in the PC, and the angles are transmitted to microcomputers. The microcomputers received the target joint angles and conduct position control of each joint.

### B. Results of Experiments

We conducted an experiment of "sinus-lifting". Sinus-lifting is a locomotion style of a snake, in which the snake lifts its body around the most bending parts during serpentine movement. It was clarified sinus-lifting prevents side slip of the body and improves efficiency of motion[1][9]. The shape of sinus-lifting is expressed by a dorsal reference curve as follows:

$$\kappa_p(s) = \frac{2\pi}{L_a}\left(-c_0\cos\frac{4\pi}{L_a}s + c_1\right) \quad (35)$$
$$\kappa_y(s) = \frac{2\pi}{L_a}\alpha\sin\frac{2\pi}{L_a}s \quad (36)$$

Here $L_a$ is wavelength, $c_0$ is a parameter related to the height of lifted parts, and $c_1$ is a parameter to compensate the shape (the curve tends to leave a level surface without $c_1$). As the result of numerical simulations, we decided the appropriate value of $c_1$ as follows:

$$c_1 = -(0.043 * \alpha^4 + 0.105 * \alpha^2)c_0 \quad (37)$$

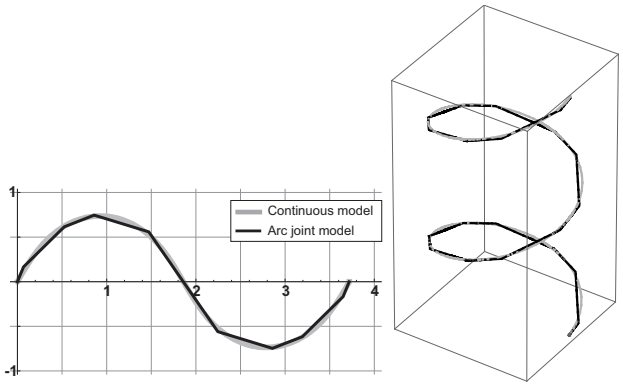


(a) Serpenoid (5 joints, $E_{nm} = 0.0036$)

(b) Spiral (10 joints, $E_{nm} = 0.0023$)

Fig. 12. Approximations by a double joint model

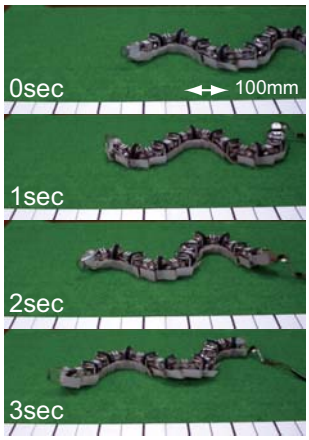


Fig. 14. The experiment of sinus-lifting

TABLE I

SPECIFICATIONS OF ACM-L2

| Size (L, W, H) | Weight | DOF | Max.torque | Joint angle |
|---|---|---|---|---|
| 800, 50, 50 [mm] | 0.99 kg | 18 | 0.5 N·m | -75∼75 deg |

Fig. 13 shows the dorsal reference curve at $\alpha = 5\pi/12$, $c_0 = 0.3$, $c_1 = -0.092$.

In this experiment, we put thin plastic plates covered with fluoride resin tape on the belly of ACM-L2 to imitate the smooth belly scales of a snake. Fig. 14 shows the experimental result when the robot approximated the shape of Fig. 13. It successfully travelled on artificial turf with velocity of 75mm/s, and it is 71% of the speed when the robot moves without slip. These scenes are contained in the attached video. The velocity of normal lateral undulation (with $c_0 = 0$) was 55 mm/s with the same condition, so the results shows sinus-lifting was conducted successfully.

## VI. CONCLUSIONS AND FUTURE WORKS

In this paper, we proposed a method of approximations to continuous curves of Active Cord Mechanism (ACM) composed of arc-shaped joints. We also discuss the similarity between an arc-shaped joint and a double joint, and proposed a method of approximations to continuous curves of ACM with double joints. The proposed method was verified by experiments of serpentine movement of a snake-like robot with double joints, and it successfully travelled with velocity of 75mm/s using sinus-lifting. This result shows the proposed method is available to generate smooth motion of ACM.

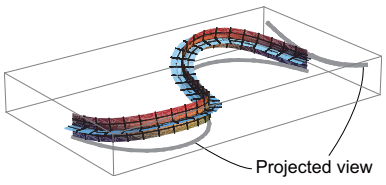


Fig. 13. A dorsal reference curve representing sinus-lifting

ACM composed of arc-shaped joints or double joints is closer to a curve than typical robots composed of straight links. At the present such kind of ACM is not major, however if a high-performance arc-shaped joint or double joint is realized, the ability of ACM will improve significantly.

## VII. ACKNOWLEDGMENTS

This research was partially supported by Ministry of Education, Science, Sports and Culture, Grant-in-Aid for Scientific Research(A), No. 18206026.

## REFERENCES

[1] S. Hirose, "Biologically Inspired Robots", *Oxford University Press*, 1993.

[2] H. Ohno, S. Hirose, " A Study of Active Cord Mechanisms -Basic Design of Pneumatically Driven Active Cord Mechanism-", *Journal of Robotics and Mechatronics*, Vol.15, No.4, pp.416-423, 2003.

[3] Bryan A. Jones, Ian D. Walker, "Practical Kinematics for Real-Time Implementation of Continuum Robots", *IEEE Transaction of Robotics*, Vol.22, No.6, pp.1087-1099, 2006.

[4] H. Yamada, S. Hirose: "Study of a 2-DOF Joint for the Small Active Cord Mechanism", *Proc. of IEEE Int. Conf. on Robotics and Automations*, pp.3827-3832, 2009.

[5] H.Yamada, S.Hirose, "Study of Active Cord Mechanism (Approximations to continuous curves of a multi-joint body)", *J. of the Robotics Society of Japan*, Vol.26, No.1, pp.110-120, 2008. (In Japanese)

[6] Gregory S. Chirikjian, Joel W. Burdick, "A Modal Approach to Hyper-Redundant Manipulator Kinematics", *IEEE Transaction on Robotics and Automation*, vol. 10, No. 3, pp343-354, 1994.

[7] M. Mori, H. Yamada, S. Hirose, "Design and Development of Active Cord Mechanism "ACM-R3" and its 3-dimensional Locomotion Control", *J. of the Robotics Society of Japan*, Vol.23, No.7, pp.886-897, 2005. (In Japanese)

[8] H. Yamada, S. Hirose, "Study on the 3D Shape of Active Cord Mechanism", *Proc. of IEEE Int. Conf. on Robotics and Automations*, pp.2890-2895, 2006.

[9] H.Yamada, S.Hirose, "Study of Active Cord Mechanism (Generalized Basic Equations of the Locomotive Dynamics of the ACM and Analysis of Sinus-Lifting)", *J. of the Robotics Society of Japan*, Vol.26, No.7, pp.801-811, 2008. (In Japanese)

[10] A. E. H. Love, "A Treatise on the mathematical theory of elasticity," *Cambridge University Press*, 1927.